

Article ID: 1003-7837(2005)02,03-0521-09

# Influence of thermomechanical processing on the structure and properties of Cu-Ag alloy *in situ* composites\*

NING Yuan-tao(宁远涛), ZHANG Xiao-hui(张晓辉), ZHANG Jie(张捷)

(Kunming Institute of Precious Metals, Kunming 650221, China)

**Abstract:** The influences of the thermomechanical processing, including the solidification conditions, the cold deformation and the intermediate annealing treatment, on the structure and properties of the Cu-10Ag alloy *in situ* composite were studied in this paper. The cast structure and the structural changes in the cold deformation and intermediate annealing process were observed. The properties including the ultimate tensile strength (UTS) and the electrical conductivity were determined. A two-stage strain strengthening effect for the Cu-10Ag alloy *in situ* filamentary composite was observed. The factors influencing the UTS and conductivity were discussed. The solidification conditions in the range of 10<sup>-3</sup>~1000 K/s cooling rates and the intermediate heat treatment showed obviously influence on the structure and properties on the Cu-10Ag alloy *in situ* filamentary composite. The typical properties of the Cu-Ag alloy *in situ* filamentary composites through thermomechanical processing were reported.

**Key words:** metal materials; composite; Cu Ag alloy; thermomechanical processing; structure; properties

**CLC number:** TG146.1, TG146.3      **Document code:** A

## 1 Introduction

The *in situ* composites based on copper alloys with high strength and high electrical conductivity has been developed for applications such as high field magnets, where the tensile strengths in excess of 1 GPa and electric conductivity above 50% IACS (International Annealed Copper Standard) are required<sup>[1-5]</sup>. The Cu alloys included essentially two types: one is the alloy system of Cu with face-centered-cubic (fcc) elements such as Ag, another is the alloy system of Cu with body-centered-cubic (bcc) elements such as Nb, Fe and Cr and so on. The Cu-Ag alloy *in situ* composites could be prepared by co-deformation of both Cu matrix and Ag phase, in which process the second phase Ag was transformed into fine filaments. The microstructure and properties of the Cu-Ag *in situ* composites have been extensively investigated and testified to be under the influence of many factors such as the content of silver, the alloying additives, the degree of deformation and intermediate heat treatment and so on<sup>[6-14]</sup>.

**Received date:** 2005-05-24

\* **Foundation item:** Project supported by the National Natural Science Foundation of China (50371031)

**Biography:** NING Yuan-tao (born in 1938), Male, Professor.

The present investigation was carried out to examine the comprehensive influence of the thermomechanical processing, including factors such as the solidification conditions, the degree of deformation and the intermediate heat treatment at lower temperature, on the evolutions of the structure and property as well as the strengthening effect of the Cu-Ag alloy. The Cu-10Ag alloy *in situ* composites with high strength and high electrical conductivities were obtained.

## 2 Experimental procedure

The 99.95%Cu and 99.99%Ag in purity were used to prepare the Cu-10%Ag (mass fraction) (simplified as Cu-10Ag) alloy. The metals were melted in an  $\text{Al}_2\text{O}_3$  crucible under the protection of pure argon gas with an induction furnace. Two ingots were got and numbered as CA1 and CA2, respectively. The ingot CA1 was solidified rapidly through pouring the alloy melt into a water-cooled copper mould, and the ingot CA2 was solidified slowly through pouring the molten alloy into a preheated graphite mould. Both ingots were cold deformed. One set of samples were directly forged and drawn to wires of 0.08 mm in final diameter, and another set of samples were experienced the lower temperature intermediate annealing at the low strain stage at first and then drawn subsequently to wires of 0.08 mm.

The samples with different true strains during deformation process were taken to measure the tensile strength and electrical conductivity and to observe the microstructure. The tensile strengths were determined using FM250 and FM3 types of machines at an initial strain rate of about  $1.0 \times 10^{-1}/\text{s}$  for wire samples with diameters  $\Phi > 0.3$  mm and  $\Phi < 0.3$  mm, respectively. The electrical resistivities were measured using a standard four-probe technique at room temperature for wire samples. The microstructure was observed using OM, SEM and TEM microscopes.

## 3 Influence of solidification conditions on microstructure

The microstructures of CA1 and CA2 alloys as cast were the dendrite crystals. The second dendrite spacing values on average were measured to be  $5 \mu\text{m}$  for CA1 alloy and  $32 \mu\text{m}$  for CA2 alloy. It is well known that the dependence of the spacing ( $\lambda, \mu\text{m}$ ) of secondary dendrite on the cooling rate ( $\dot{\epsilon}, \text{K/s}$ ) in the solidification process is an exponential function and can be expressed as:

$$\lambda = B \cdot \dot{\epsilon}^{-n} \quad (1)$$

where,  $B$  is a coefficient related to alloy system and takes the unit of  $\mu\text{m} \cdot \text{K}^n \cdot \text{s}^{-n}$ ,  $n$  is the exponential related to alloy system. For the Cu alloys with higher copper content,  $B = 160 \mu\text{m} \cdot \text{K}^{0.4} \cdot \text{s}^{-0.4}$  and  $n = 0.4$ <sup>[15]</sup>. So, the  $\dot{\epsilon}$  values could be calculated according to formula (1) and were  $\dot{\epsilon}(\text{CA1}) = 5.8 \times 10^3 \text{ K/s}$  for CA1 alloy and  $\dot{\epsilon}(\text{CA2}) = 57 \text{ K/s}$  for CA2 alloy, respectively. The cooling rates of the two solidification conditions differ by two orders of magnitude.

The microstructure of the cast Cu-10Ag alloy consisted of the Ag precipitate, the (Cu+Ag) eutectic and the Cu phase. Changing the solidification conditions did not change the compositions of the structural phases but altered the proportions of the phases in both as-cast alloys, as shown in Table 1. It can be seen that the proportion of the Ag precipitate phase in CA2 alloy was three times higher than that in CA1 alloy, but the proportion of (Cu+Ag) eutectic in CA1 alloy was two times higher than that in CA2 alloy. It indicated that the rapid solidification restrained the separation of the Ag precipitate phase and increased the proportion of the (Cu+Ag) eutectic, and that the slow solidification improved inversely the separation of the primary Ag precipitate phase.

**Table 1** Phase proportions in the as cast Cu-10Ag alloys under different solidification conditions

Alloy number	Solidification Conditions	Cooling rate / (K · s <sup>-1</sup> )	Cu phase / %	(Cu+Ag) eutectic / %	Ag precipitate phase / %
CA1	In water cooling copper mould	5.8 × 10 <sup>3</sup>	69.1	30.2	0.7
CA2	In preheated graphite mould	57	81.0	16.5	2.5

Figure 1 showed the dendrite morphology and distribution of the structural phases in the as-cast Cu-10Ag alloy. It can be seen from Figs. 1(a) and (b) that the size and spacing of the dendrite crystals of CA1 alloy solidified rapidly were obviously smaller than those of CA2 alloy solidified slowly. In Fig. 1(c), the black regions were the essentially pure copper matrix and surrounded by the Ag precipitate films, which were about 0.5–1.0 μm width for CA1 alloy and 1.5–2.0 μm width for CA2 alloy. The (Cu+Ag) eutectic colonies were distributed in the interdendritic zones (gray white E zones) and adjacent to the Ag rings. The sizes of Ag lamellae in the eutectic colonies were much finer than the primary Ag precipitate films. The observation is consistent with that of Sakai *et al.* [4]

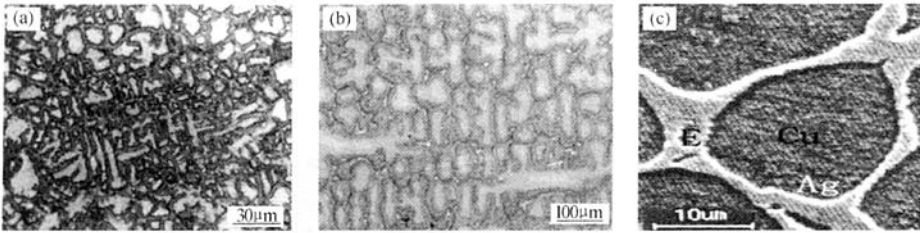


**Fig. 1** Dendrite morphology and distribution of the structural phases in the cast Cu-10Ag alloy  
(a)–CA1 alloy; (b)–CA2 alloy; (c)–CA1 alloy

## 4 Influence of deformation degree on microstructure and properties of the Cu-10Ag alloy

### 4.1 Microstructure evolution in the deformation processing

In the deformation process, the Ag phase including the Ag precipitates and the Ag lamellae in the eutectic colonies were transformed into Ag fibers (Fig. 2). The Ag precipitates were developed into relatively coarse fibers, whereas the Ag lamellae in the eutectic colonies were transformed to relatively fine filaments.

The diameters of the Ag fibers, formed from the Ag precipitates in the different true strain stages, were measured by SEM observation and showed in Fig. 3. It was found that the diameters(*d*) of the Ag fibers could be approached through an exponential function of the true strain ( $\eta$ ):  $d=C \cdot \exp(-0.228\eta)$ , where *C* is a coefficient related to the size of the original crystals and was 900nm for CA1 alloy and 1500nm for CA2 alloy in the present case, respectively. So, the Cu-10Ag alloy solidified rapidly had finer and denser silver filaments throughout the final wires.

Fig. 4(a) indicated further that the Ag filaments in

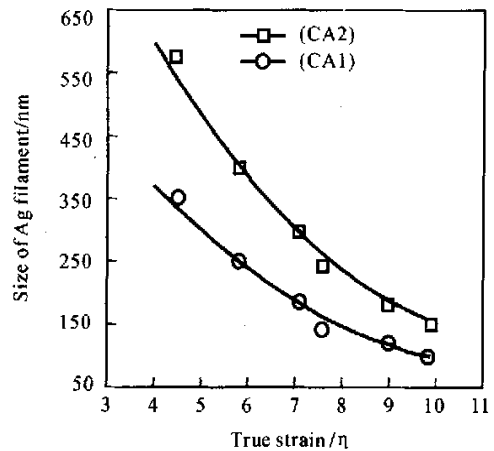


**Fig. 3** Dependences of average diameters of Ag fibers on the true stain for CA1 and CA2 alloys

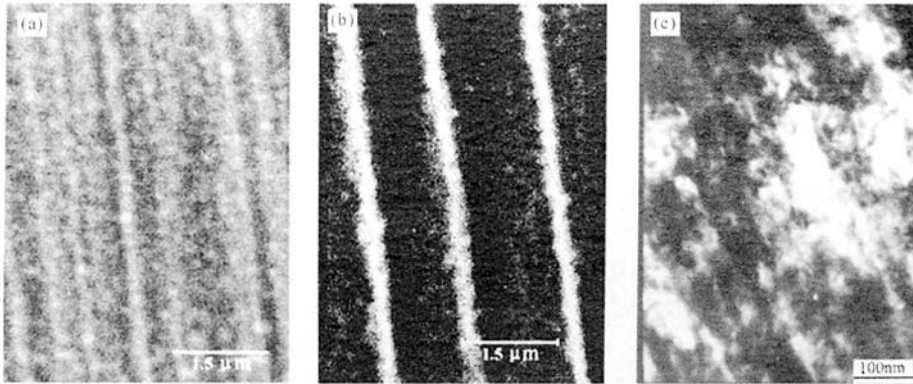


Fig. 2 SEM micrograph of Ag fibers in CA1 and CA2 Alloys as  $\eta=7.1$  (a, b), respectively, and TEM micrograph of the CA1 alloy ribbon as  $\eta=10.4$  (c)

the heavy deformed Cu-10Ag alloy were in a dislocation-free state. The Kikuchi line in Cu matrix shown in Fig. 4 (b) indicated also a state with low density of defects. Figs. 4(c) and (d) were electron diffraction patterns correspond to the points a and b noted in Fig. 4(a), in which the texture with a cube-to-cube orientation relationship  $(\bar{1}11)_{Cu} \parallel (\bar{1}11)_{Ag}$ ,  $[110]_{Cu} \parallel [110]_{Ag}$  between Cu matrix and Ag filament was observed, as shown in Figs. 4(d, d).

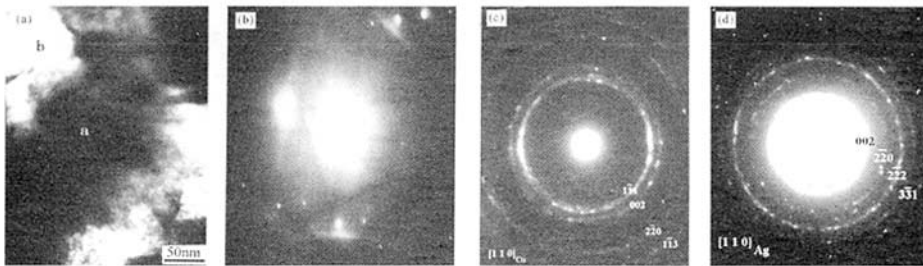


Fig. 4 TEM micrograph (a), the Kikuchi line (b) and electron diffraction patterns (c, d) for the CA1 alloy with the true strain  $\eta=10.4$ .

#### 4.2 Properties of the deformed Cu-10Ag alloy *in situ* composite wires

Fig. 5 showed the dependences of the ultimate tensile strength (UTS) on the true strain for CA1 and CA2 alloy *in situ* composite wires. The UTS values increased with increase of the true strain. At lower true strain stage as  $\eta < 8.5$ , however, the UTS values of CA1 alloy were lower than those of CA2 alloy; at higher true strain stage as  $\eta > 8.5$ , the UTS values of CA1 alloy increased rapidly and were higher than those of CA2 alloy.

The evolution of UTS in the deformation process showed a two-stage strain strengthening effect. At low strain stage, the dislocation cells with about 150–200 nm occurred<sup>[13]</sup>, and the dislocation density in the Cu matrix and the Ag phase,  $\gamma_{d(Cu)}$  and  $\gamma_{d(Ag)}$ , should increase with the deforming degree and could reach  $10^{12} - 10^{14} \text{ cm}^{-2}$ <sup>[18]</sup>. According to the model of dislocation piling, the strengthening to the composite was controlled mainly by the work hardening or dislocation strengthening in Cu matrix and Ag phase and directly proportional to  $\sqrt{\gamma_{d(Cu)}}$  and  $\sqrt{\gamma_{d(Ag)}}$ . The sizes of the Cu grains and Ag filaments in CA2 alloy were much larger than that in CA1 alloy (Fig. 3). It could be considered that the CA2 alloy can contain more dislocation cells and higher dislocation density than the CA1 alloy, namely  $\gamma_{d(CA2)} > \gamma_{d(CA1)}$ . On the other

hand, CA2 alloy contained higher proportion of Ag precipitate than CA1 alloy. So the CA2 alloy possessed higher strength than the CA1 alloy. At higher strain stage, the superfine Ag filaments could not contain the stable dislocation cells. The dislocations or the dislocation cells generated at low strain stage should migrate out of Ag filaments and turned into grain boundaries. The Ag filaments were in a dislocation-free

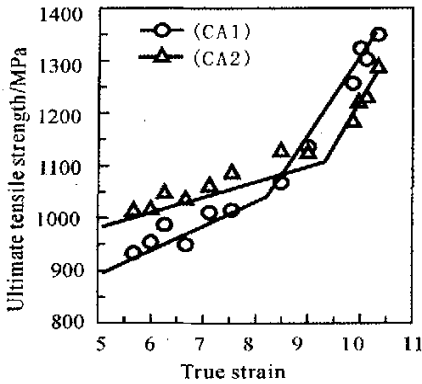


Fig. 5 Dependence of UTS on true strain for both CA1 and CA2 alloys

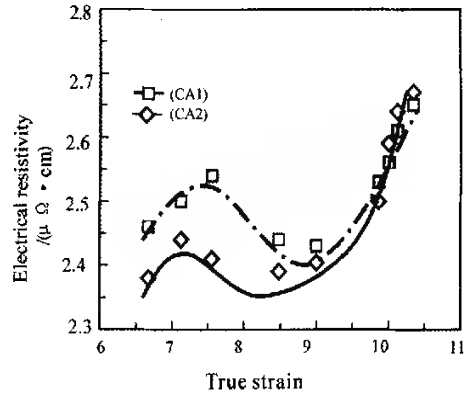


Fig. 6 Dependence of resistivity on true strain for both CA1 and CA2 alloys

state. The Cu matrix was also in a state with low density of defects (Fig. 4(b)). So, the strengthening to heavy deformed composite was mainly dependent to mechanism caused by superfine Ag filaments or the large interfaces. The strengthening mechanism made the UTS increase rapidly. Because the sizes of both the Ag filaments and the Cu grains in CA1 alloy were much smaller than that in CA2 alloy, so the CA1 alloy possessed higher strength than CA2 alloy at high true strain stage. The similar two-stage strain strengthening effect in Cu-Ag alloy *in situ* composites were also observed by other authors<sup>1,13</sup>.

Fig. 6 showed the dependence of the electrical resistivity on the true strain for both CA1 and CA2 alloys. It presented also two stage changes with increase of the true strain. At the low strain stage, the resistivity increased at first then had smaller fluctuation of about  $1 \mu\Omega \cdot \text{cm}$ . It means that the dislocation density in both alloy increased firstly due to the true strain increasing and then decreased due to the dislocation migrating out. At the high strain stage, the resistivity increased rapidly due to the Ag filamentary refining highly and the interface area increasing. The changes of the resistivity for both alloys were based on the same structural reason and mechanism as that of the strengthening effect.

## 5 Influence of intermediate heat treatment on the microstructure and properties

### 5.1 Microstructure evolution in the heat treatment process

The annealing treatment of the cold deformed Cu-10Ag alloy promoted the separation of the Ag precipitate. The morphology and the size of the Ag precipitate were related to the annealing temperature. The composite aged at the temperatures below  $200^\circ\text{C}$  maintained still the highly filamentary structure, but a similar separating process of Ag precipitate was observed at temperatures above  $200^\circ\text{C}$  for CA1 and CA2 alloys. Aging 1 hour at  $200^\circ\text{C}$ , the very fine Ag precipitate grains with size of about 2–8 nm separated from the Cu matrix (Fig. 7(a)). Aging at  $300^\circ\text{C}$ , the layered Ag precipitate formed (Fig. 7(b)) and the partial Ag precipitate began to be spheroidized (Fig. 7(c)). At  $400^\circ\text{C}$  aging, the spheroidized Ag precipitate grew up (Fig. 7(d)), the partial recrystallization occurred. The alloys were recrystallized well at  $500^\circ\text{C}$  aging. With

the annealing temperature rising, the lattice constants of CA1 and CA2 alloys were reduced slowly as below 300°C and quickly as above 300°C.

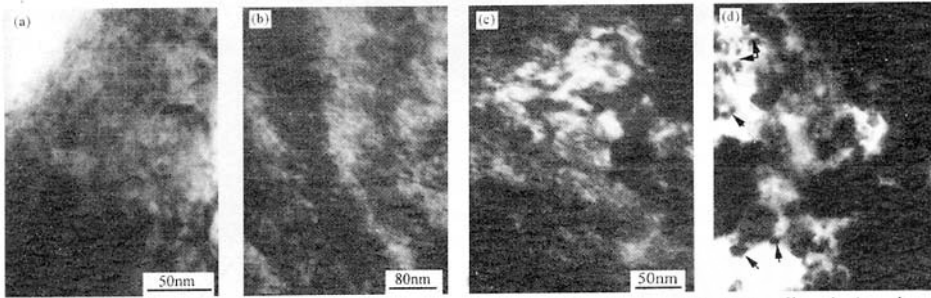


**Fig. 7** Morphology and distribution of the Ag precipitate of the deformed Cu-10Ag alloy during the annealing process at different temperatures  
(a)–200°C; (b)–300°C; (c)–300°C; (d)–400°C

## 5.2 Influence of intermediate heat treatment on properties of the Cu-10Ag alloy composites

### 5.2.1 Aging strengthening effect of the cold deformed Cu-10Ag alloy

The influences of the annealing temperature on the properties of the Cu-10Ag *in situ* filamentary composite depended on the cold deformation degree and the annealing temperature. Fig. 8 showed the influence of the annealing temperatures on the properties of the deformed Cu-10Ag alloy with the true strain  $\eta=6.0$ . With the annealing temperature rising, the UTS values of CA1 and CA2 alloys increased at first and then decreased after about 350°C. The conductivities of both alloys increased lightly at first and then rapidly after about 300°C. It indicated that the Cu-10Ag *in situ* filamentary composites showed important aging strengthening effect and possessed improved conductivity during the annealing process. Obviously, the separation of the Ag precipitate is responsible for the aging strengthening effect. On the other hand, the separation of the Ag precipitate led to the decrease of the solid solubility of Ag in the Cu matrix and the increase of the quantity of Ag phase, it made the electrical conductivity increase, especially for the alloy annealed at high temperature.

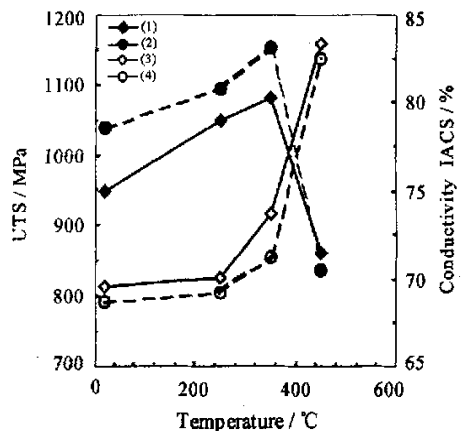


**Fig. 8** Effect of the annealing temperatures on strength (curve 1, 2) and conductivity (curve 3, 4) of Cu-10Ag alloy deformed with the true strain  $\eta=6.0$  (1), (3)–CA1 alloy; (2), (4)–CA2 alloy;

### 5.2.2 Influence of the intermediate heat treatment on properties of the heavy deformed composite wires

Fig. 9 showed the influence of IAT at 350°C for 1 hour at  $\eta=2.95$  on the UTS and conductivity of CA1 and CA2 alloys deformed heavy with the true strain  $\eta=10.4$ . It can be seen that the IAT increased obviously the UTS values of the composite wire but maintained still high conductivities. Table 2 listed some typical data of the UTS and the relative conductivity of the CA1 and CA2 alloy composite wires. Here, IACS is the relative conductivity of the Cu-10Ag alloy to the international annealing copper standard and is equal to  $\rho(\text{Cu})/\rho(\text{Cu-10Ag}) \times 100\%$  with  $\rho(\text{Cu})=1.69\mu\Omega \cdot \text{cm}$ . It is clear that the highest UTS values of 1560 MPa and 1500 MPa with conductivities of 64% and 62% IACS could be obtained for the heavy deformed CA1 and CA2 alloy *in situ* filamentary composite wires experienced the IAT at lower true strain,

and that the *in situ* filamentary composite based on the Cu-10Ag alloy solidified rapidly possessed higher UTS values than that based on the alloy solidified slowly.

As mentioned above, the intermediate annealing treatment of the deformed Cu-10Ag alloy promoted the separation of Ag precipitate. The separated Ag precipitate grains or spheroids were subsequently re-drawn and transformed into very fine Ag filaments. So, the heavy drawn Cu-10Ag *in situ* filamentary composite wire with IAT had finer and denser Ag filaments than that without IAT. It is the reason why the IAT increased obviously the UTS of the *in situ* filamentary composite wires.

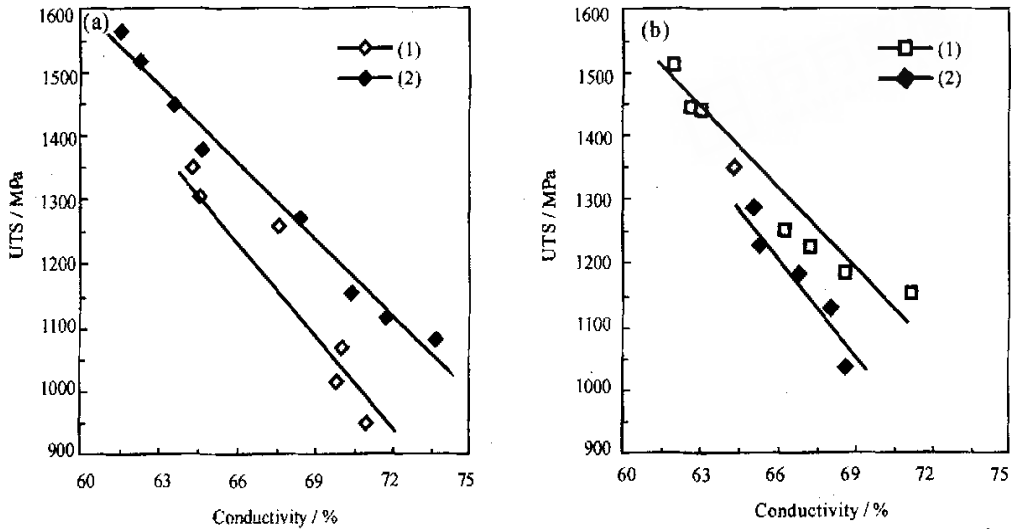


**Fig. 9** UTS vs conductivity for CA1(a) and CA2(b) alloys *in situ* filamentary composite wire  
 Curve 1: The composite wire heavy deformed directly with true strain  $\eta=10.4$  without IAT; Curve 2: The composite wire experienced 1 IAT at 350°C for 1 hour at  $\eta=2.95$  and followed through heavy deformation with true strain  $\eta=10.4$

**Table 2** Influence of the thermomechanical processing on the properties of Cu-10Ag alloy composite wires

Thermomechanical processing	CA1 alloy composite wire		CA2 alloy composite wire	
	UTS/MPa	Conductivity/%IACS	UTS/MPa	Conductivity/%IACS
$\eta=10.4$ , without IAT	1355	64	290	64
$\eta=10.4$ , with IAT <sup>1)</sup>	1560	62	1500	63

Note: 1) IAT= annealing at 350°C for 1 hour at  $\eta=2.95$

## 6 Conclusions

The Cu-10Ag alloys with cooling rates of 10–1000 K/s were prepared. The structural phases of the alloys as cast consisted of the Ag precipitate, the (Cu+Ag) eutectic and Cu phase. Changing the solidification conditions could alter the proportions of the phases. The rapid solidification restrained the separation of the Ag precipitate phase, increased the portion of the (Cu+Ag) eutectic and refined the original grains of various phases; but the slow solidification improved the separation of the Ag precipitate phase.

In the deformation process, the Cu-10Ag alloy was developed to the *in situ* filamentary composite. The Ag precipitate in the cast structure were developed into relatively coarse Ag fibers, the diameters(*d*) of which can be approached through an exponential function of the true strain( $\eta$ ):  $d=C \cdot \exp(-0.228\eta)$ ,

whereas the Ag layers in the eutectic colonies were transformed to very fine Ag filaments with about a few nanometers in diameter. The Ag filaments were in the dislocation-free state and the Cu matrix was in a state with low density of defects for the Cu-10Ag alloy *in situ* composite heavily deformed with the true strain  $\eta \geq 9$ . Based on the same structure evolution, the ultimate tensile strengths of the composite increased and the conductivities decreased with increase of the true strain. The Cu-Ag alloy *in situ* filamentary composites contained a two-stage strain strengthening effect. At low strain stage, the strengths of the alloy composite wires were controlled mainly by the work hardening mechanism in Cu matrix and Ag phase, and the strengthening rate of the alloy solidified rapidly was lower than that of the alloy solidified slowly. At high strain stage, the strengths of the composite wires were mainly dependent to the strengthening mechanism of superfine Ag filaments or the large interfaces, and the strengthening rate of the alloy solidified rapidly was higher than that of the alloy solidified slowly.

The annealing of the deformed Cu-10Ag alloy *in situ* composites promoted the separation of fine Ag precipitate and the aging strengthening effect, which were related to the annealing temperatures. The intermediate heat treatment at the low strain stage during the heavy deformation process refined the Ag filaments, increased the ultimate tensile strength and the electrical conductivity of the Cu-10Ag *in situ* filamentary composites.

So, the suitable thermomechanical processing is an important condition to obtain the optimum comprehensive properties for the Cu-Ag alloy *in situ* filamentary composite. For example, the typical comprehensive properties could be reached to UTS of 1560 MPa for the rapidly solidified alloy and to UTS of 1500 MPa for the slowly solidified alloy with conductivities of 62%–64% IACS.

#### Acknowledgement

This project was supported by the National Natural Science Foundation of China under Grant of No. 50371031.

#### References

- [1] Sakai Y, Inoue K, Asano T. Development of high strength high conductivity Cu-Ag alloy for pulsed magnets[J]. IEEE Trans Magn, 1992, 28(1): 888.
- [2] Dew-Hughes D. High strength conductor for pulsed magnets[J]. Mater Sci Eng, 1993, A168:35.
- [3] Sakai Y, Inoue K, Maeda H. New high-strength, high-conductivity Cu-Ag alloy sheets[J]. Acta Metall Mater, 1995, 43(4): 1517.
- [4] Sakai Y, Schneider-Muntau H J. Ultra-high strength, high conductivity Cu-Ag alloy wires[J]. Acta Mater, 1997, 45(3): 1017.
- [5] Ning Y T, Zhang X H, Zhang J. Stability of the heavy deformed Cu-Ag alloy *in situ* Filamentary Composites[J]. Trans Nonferrous Met Soc China, 2005, 15(4):506.
- [6] Ning Y T, Zhang X H, Qin G Y Zhang J. Structure and properties of the *in situ* filamentary composites based on the Cu-Ag alloy with different solidification conditions [J]. Precious Metals, 2005 26(3):46.
- [7] Zhang X H, Ning Y T, Li Y N, *et al.* Properties of heavy deformed Cu-Ag alloy *in situ* composites[J]. Trans Nonferrous Met Soc China, 2003, 12(1): 115.
- [8] Hong S I, Hill M A, Sakai Y, *et al.* On the stability of cold drawn two-phase wires[J]. Acta Metall Mater, 1995, 43(9): 3313.
- [9] Hong S I, Hill M A. Microstructural stability and mechanical response of Cu-Ag microcomposite Wires[J]. Acta Mater, 1998, 46(12): 4111.
- [10] Hong S I, Hill M A. Mechanical stability and electrical conductivity of Cu-Ag filamentary microcomposites[J]. Mater Sci Eng, 1999, A264: 151.
- [11] Han K, Vasquez A A, Xin Y, *et al.* Microstructure and tensile properties of nanostructured Cu-25wt% Ag[J].

- Acta Mater. 2003, 51:767.
- [12] Morris D G, Benghalem A, Morris-Munoz M A. Influence of solidification condition, thermomechanical processing, and alloying additions on the structure and properties of *in situ* composite Cu-Ag alloys[J]. Scripta Mater, 1999, 41(10): 1123.
- [13] Benghalem A, Morris D G. Microstructure and strength of wire-drawn Cu-Ag filamentary composites[J]. Acta Mater, 1997, 45(1): 397.
- [14] Han K, Embury J D, Sims J R, *et al.* The fabrication properties and microstructure of Cu-Ag and Cu-Nb composite conductors[J]. Mater Sci Eng, 1999, A267: 99.
- [15] Jones H. The status of rapid solidification of alloy in research and application[J]. J Mater Sci, 1984, 19(4): 1043.
- [16] Frommeyer G, Wassenmann G. Microstructure and anomalous mechanical properties of *in situ* produced silver-copper composite wire[J]. Acta Metall, 1975, 23: 1353.